Published in final edited form as:
Calcif Tissue Int. 2010 June ; 86(6): 484–494. doi:10.1007/s00223-010-9365-0.

Changes in bone micro-architecture and biomechanical properties in the *th3* thalassemia mouse are associated with decreased bone turnover and occur during the period of bone accrual

Maria G. Vogiatzi[1], **Jaime Tsay**[1], **Kostas Verdelis**[2], **Stefano Rivella**[1], **Robert W Grady**[1], **Stephen Doty**[2], **Patricia J Giardina**[1], and **Adele L Boskey**[2]

[1] Department of Pediatrics, Weill Cornell Medical College, 525 East 68th Street, New York, NY 10065

[2] The Hospital for Special Surgery, 535 East 70th Street, New York, NY 10021

Abstract

Osteoporosis and fractures occur frequently in patients with beta thalassemias, a group of congenital hemolytic anemias characterized by decreased synthesis of the beta chain of hemoglobin. In this study, we determined the bone abnormalities of the *th3* thalassemia mouse, generated by deletion of the mouse beta chain genes. The heterozygote *th3*/+ mouse has moderate anemia, and serves as a model of beta thalassemia intermedia (TI), which represents the mild thalassemia phenotype. The *th3/th3* mouse has lethal anemia and is a model of beta thalassemia major (TM), which is characterized by life-threatening anemia requiring regular transfusions to sustain life.

Compared to controls: i) Micro-CT of trabecular bone showed decreased bone volume fraction, number of trabeculae and trabecular thickness in both *th3*/+ and *th3/th3* ($p<0.05$). ii) Cortical bone analysis showed thinner cortices and increased marrow area in *th3*/+ animals ($p<0.05$). iii) Micro-CT abnormalities in *th3*/+ mice were present by 2 months and did not worsen with age. iv) Histomorphometry was significant for decreased bone formation and resorption in both *th3*/+ and *th3/th3*. Similarly, cathepsin K and osteocalcin expression from bone of both *th3*/+and *th3/th3* animals was reduced ($p<0.05$). vi) Biomechanics showed reduced maximum load, maximum moment and structural stiffness in both *th3*/+and *th3/th3* ($p<0.01$).

In conclusion, the *th3 mo*use model of thalassemia manifests bone changes reminiscent of those in humans, and can be used for further bone studies in thalassemia. Bone changes are associated with decreased bone turnover, and develop early on during the period of bone accrual.

Introduction

Beta thalassemia is a group of congenital hemolytic anemias characterized by the absence or decreased synthesis of the beta chain of hemoglobin [1]. Depending on the severity of the anemia, patients may require periodic or regular transfusions to sustain life. The paradox of life saving transfusion therapy is progressive transfusional iron overload, which leads to multiple endocrine complications, and has lethal hepatic and/or cardiac consequences. Iron

Corresponding Author: Maria G Vogiatzi, MD, Weill Cornell Medical College, Pediatric Endocrinology, Box 103, 525 East 68th Street, New York, NY 10065, Tel: 212-746-3462, Fax: 212-746-8261, mvogiatz@med.cornell.edu.

chelation therapy, introduced in the mid 1970's, has reduced these complications and prolonged survival [1,2].

Osteoporosis has been recognized as a frequent problem in thalassemia, affecting most of the patients [3–7]. Incidence of fractures is also increased compared to the general population, and rates correlate with the severity of osteoporosis [3,7]. The etiology of low bone mass is considered multi-factorial. Ineffective erythropoiesis, characterized by the production of large number of defective erythroids is thought to lead to medullar expansion and cortical thinning. However, osteoporosis occurs frequently despite regular transfusions and near normalization of hemogolin concentrations begenning early life. In addition, iron overload, chelation, and endocrine dysfunction secondary to iron overload have all been implicated in the development of low bone mass. However, recent studies in humans have yet to identify with certainty the exact role of each of these factors [7].

Studies on the bone disease of thalassemia using a mouse model have not yet been performed. The recent development of the thalassemia mouse (*th3*) can provide a tool for study of this disease [8]. This mouse was generated by deletion of both mouse beta globin genes, *b1* and *b2*, located on chromosome 7 of the C57/BL6 mouse [8]. In this study, we sought to characterize the bone abnormalities that occur in the *th3* thalassemia mouse. From these results and further manipulation of this model, we hope to shed light on the etiology of low bone mass in thalassemia as a prelude to developing more effective therapies.

In humans, the most severe form of homozygous beta thalassemia, called beta thalassemia major (TM) or Cooley's anemia, is characterized by a life-threatening anemia, which results in death if not treated by chronic transfusions [1]. A less severe phenotype, beta thalassemia intermedia (TI), is associated with mild to moderate anemia that does not require regular transfusions[1]. The heterozygous *th3* mouse (*th3/+)* exhibits a phenotype comparable to human beta TI, which is characterized by moderate anemia. The homozygous *th3* mouse, (*th3/th3*), dies late in gestation because the switch from fetal to adult hemoglobin production is completed between gestational days 14 and 16, while in humans, the switch occurs in early childhood. An adult mouse model of beta TM was generated by engrafting wild-type (WT) C57/BL6 mice with beta-globin-null (*th3/th3*) fetal liver cells(FLCs)[8]. This engrafted mouse, referred here as *th3/th3*, manifests a lethal red cell hemolysis approximately 2 months post transplant. It was used in this study to investigate the bone changes characteristic of beta TM.

Material and Methods

Animals

Th3/+ mice were generously provided by Dr. Rivella's laboratory. Engrafted *th3/th3* mice were generated as previously described (8). Two-month-old WTC57/BL6 recipient mice were irradiated (IR) with 9 Gy (single dose) and transplanted with donor *th3/th3* fetal liver cells on the day of irradiation. Donor fetal liver cells were harvested at embryonic day 14.5 from embryos obtained by intercrossing *th3/+* mice. The genotype of the embryos was determined by analyzing their hemoglobin(Hb)by cellulose acetate electrophoresis. A second group of 2-month-oldC57/BL6 mice was irradiated and transplanted with fetal liver cells from WT embryos and served as irradiated controls (IR) for experiments involving *th3/th3* mice. All studies were approved by the Institutional Animal Care and Use Committees of Weill Cornell Medical College.

Experimental Design and procedures

i) Characterization of the bone phenotype of the thalassemia mouse—To determine the bone abnormalities of the *th3/th3* mouse, we studied its changes compared to IR and WT controls. *th3/th3* and IR animals were generated as described above at age 2 months. They were sacrificed 2 months post transplantation, at age 4 months. The WT control group consisted of sex matched C57/BL6 mice, also sacrificed at age 4 months(n= 6 per group, 3M/3F). To characterize the *th3/+* mouse, we studied its bone abnormalities compared to age and sex matched C57/BL6 controls (6 per group, 3M/3F) at age 4 months.

The vertebrae and right femur from each animal were cleaned of soft tissue, stored in 90% ethanol, and scanned by Micro-Computed Tomography(μCT)as detailed below. After μCT analysis, the femurs were subjected to biomechanical testing as described below. For dynamic histomorphometry, mice were injected with calcein (100 mg/kg body wt) and xylenol orange (90 mg/kg body wt), respectively, at 7 and 3 days prior to sacrifice. The left femur was fixed in graded ethanols and embedded in methyl methacrylate (MMA). Longitudinal non-decalcified femur sections (5 μm) were cut on a HM360 microtome (Microm, Walldorf, Germany) and used for histomorphometry, as detailed below. Additional longitudinal non-decalcified sections (2 μm) were mounted on barium fluoride (BaF_2) infrared windows (Spectral Systems, Hopewell Junction, NY) for Fourier transform infrared spectroscopic imaging (FTIRI) analyses. One femur from a second set of *th3* and *th3/th3* animals (n=6/group) fixed in 10% buffered formalin at 4°C, dehydrated in progressive concentrations of ethanol, cleared in xylene, and embedded in paraffin. Five-micron thick sections were cut, deparaffinized and stained for tartrate-resistant acid phosphatase (TRAP). The other femur was cleaned, the tips were cut and bone marrow was removed. The remaining bone was used for mRNA extraction as described below. Liver and spleen were collected for measurement of tissue iron content.

ii) Longitudinal studies of the *th3/+* mouse—To determine if the bone abnormalities in this mouse model of thalassemia worsen with age, we performed longitudinal μCT studies of the *th3/+* mouse. *Th3/+* mice and age-matched C57/BL6 controls (6 per group, 3M/3F) were also studied at 2, 6 and 9 months of age. Similar studies could not be performed with the *th3/th3* mouse, because it dies of anemia 2 months after transplantation. The vertebrae and right femur from each animal were cleaned of soft tissue, stored in 90% ethanol, and scanned by μCT as detailed below. Liver and spleen were removed for measurement of tissue iron content.

Hemoglobin and Tissue Iron Content

Hemoglobin (Hb) measurements were made using the HemoCue Hemoglobin System (Lake Forest, CA) prior to sacrifice. Spleen and liver iron content was determined by atomic absorption spectroscopy. Whole organ weight was determined and a representative sample placed in a tarred porcelain crucible. After determining the wet weight of the sample, the crucible was placed in a drying oven (110 °C)overnight. The dry weight of the sample was determined after which it was ashed in a Muffle furnace at 550 °C. The ash was dissolved in 3N HCl, and its Fe content determined by atomic absorption.

Micro-Computed Tomography (μCT)

Densitometry and morphometry μCT analysis was performed on cortical bone from mid-diaphyses of femurs and trabecular bone from distal femurs and L5 vertebrae. Bones were scanned in their entirety by two different microCT scanners. The Enhanced Vision Systems (GE Healthcare; London, Ontario, Canada) model MS08 was used on mice aged 2 and 4 months and the model MS09 on those aged 6 and 9 months. An isotropic 12 × 12 × 12 μm voxel size was used in the 2 and 4 month-old mice bone scans and a 15 × 15 × 15 μm voxel

size was used in the 6 and 9 month-mice bone scans. 80KVp, 80 μAmperes and 4° rotation step were used in all scans. Reconstruction of 3D volumes from the 2D projections into CT volume data was performed using Beam software (GE Healthcare) with a modified Parker algorithm. Densitometric analysis of the 3D volumes was performed using microView software (GE Healthcare). For morphometric analysis the Scanco software was used (Scanco Medical, Basserforf, Switzerland).

Cortical and trabecular regions of interest (ROIs) were first defined on the volumes of the whole bones using a utility of the microView software. In the femurs, the trabecular ROIs extended from 50 um proximally to the end of the distal growth plate over 1.7mm towards the diaphysis. The whole trabecular bone was included for analysis in vertebral bodies. Trabecular ROIs were free-hand drawn on sequential slices to include the endosteal envelope, conforming to the endosteal contour on each slice. Cortical ROIs were defined as 1.7mm segments of the mid-diaphysis the femurs. A global threshold was defined as the lowest mineral density, from all bones analyzed, for which volumes were noise-free and trabeculae appeared to have the same width in binarized images as in the grayscale image. Bone mineral density (BMD) measurements were performed on cortical and trabecular volumes after segmentation of bone voxels using the global threshold, to only include bone tissue. For cortical and trabecular morphometry measurements, the volumes were binarized using the same threshold as in the BMD measurements. They were then exported as DICOM files for processing by the SCANCO software. Bone Morphometric variables of cortical bone regions included bone area and thickness, inner and outer perimeter, marrow area, maximum cross-sectional moment of inertia (I_{max}) and minimum cross-sectional moment of inertia (I_{min}). The morphometric parameters defining trabecular bone included, directly measured in 3 D, bone volume fraction (BV/TV), trabecular thickness (Tb.Th.), trabecular number (Tb.No.), and trabecular spacing (Tb.Sp.).

Fourier Transformed Infrared Imaging Spectroscopy (FTIRI)

Three sections of proximal femur from each animal were examined by FTIRI using the Perkin Elmer Spotlight 3.0 Imaging system (Perkin Elmer Instruments; Shelton, CT). Cortical and trabecular bone were examined separately. The spectral resolution was either 4 or 8cm^{-1}, while the spatial resolution was ~7 μm. Spectra were transformed to yield images corresponding to infrared band areas, peak height ratios, and integrated area ratios by a combination of the spectrometer software and ISYS Chemical Imaging Software (v 2.1; Spectral Dimensions; Olney, MD, USA). Background spectra were collected under identical conditions from the same BaF_2 windows.

Three spectroscopic parameters were calculated: mineral-to-matrix ratio, carbonate -to-mineral ratio, and collagen cross-link ratio. The mineral-to-matrix (Min/Matrix) is the integrated areas ratio of the PO_4 band [900–1200 cm^{-1}]to amide I band [1590–1720 cm^{-1}] and a measure that corresponds to ash weight [9]. Carbonate-to mineral (Carb/Min) ratio (carbonate band [840–890cm^{-1}]/PO_4 band [900–1200 cm^{-1}])indicates carbonate substitutions in hydroxyapatite [10]. The collagen cross-link (Crosslink) ratio is a parameter reflecting the relative ratio of nonreducible and reducible collagen cross-links, expressed as the absorbance ratio at two specific wavelengths (1660 and 1690 cm^{-1}) [11]. In the spectral images, pixels devoid of bone (no mineral and/or matrix spectral signature) were set to zero and masked so as to be excluded from the calculations. The spectroscopic results were expressed as histograms describing the pixel distribution of the parameters above resulting in 3 cortical and 3 cancellous bone parameters for each bone. Means for each animal's cortical and trabecular bone was calculated, along with characteristics of the pixel distributions generated at the same time using ISYS software(Olney, MD). Means and SDs were averaged for multiple sites in each animal and among the six different animals for each age and genotype using Microsoft EXCEL.

Bone histomorphometry

Longitudinal femur sections were stained using the von Kossa method and Goldner's trichrome. Bone measurements were performed in cancellous bone tissue of the proximal metaphysis beginning 1 mm from the central region of the growth plate to exclude the primary spongiosa and 500 μm from the endocortical margins to exclude modeling bone. The Bioquant program (Bioquant-True Color Windows, Advanced Image Analysis Software, sVGA Frame Grabber Image Processing Board and Optronics DEI-470 Video Camera) was used to collect the raw data. Trabecular bone volume (BV/TV, %), osteoclast surface and osteoid surface for Bone Surface (BS) were measured. Paraffin embedded longitudinal tibia sections were stained for tatrate-resistant acid phosphatase (TRAP) using a commercially available kit (Sigma, St Louis, MO). Osteoclasts were identified as TRAP positive cells on the bone surface. Osteoclast number per BS (no/mm) was then determined using the same Bioquant program.

Fluorocrhome-based indices of bone formation were measured in unstained 5μmlongitudinal sections of distal femur. Double and single labeled perimeters were identified. Interlabel widths of double labeled regions were measured using the Bioquant program. The mineral apposition rate (MAR, μm/day)and bone formation rate (BFR/BS, $\mu m^3/\mu m^2$/day) were then determined.

Biomechanical Testing

The structural mechanical behavior was measured via three-point bending to failure. The femur, with the anterior aspect facing up, was placed horizontally on two supports with a span width of 7.0mm. A central load was applied on the anterior surface of the mid-diaphysis midway between the supports at a displacement rate of 0.05 mm/s using an ElectroForce 3200 system (BOSE, Eden Prairie, MN)until the bone fractured. Maximum load, structural stiffness and maximum moment were determined from the resulting load-displacement curve. Structural stiffness was calculated as the slope of the linear ascending portion of the curve.

Quantitative RT-PCR

mRNA from femurs of *th3/+* and *th3/th3* animals and their controls was extracted after bone marrow was removed. Total RNA was prepared from the tibia using TRIzol reagent (Sigma-Aldrich; St. Louis, MO) according to the manufacturer's instructions. First-strand cDNA was synthesized with a SuperScript First-Strand Synthesis System for RT-PCR using SuperScript II reverse transcriptase enzyme (Invitrogen; Carlsbad, CA). All reactions were performed in a Chromo4 thermocycler (MJ Research, Waltham, MA) using FastStart SYBR Green Master Mix (Roche; Indianapolis, IN). The primers used for expression analysis, cathepsin K (CTK; forward, 5′-CAGCAGGATGTGGGTGTTCA-3′ and reverse, 5′-ACACTGGCCCTGGTTCTTGA-3′), osteocalcin (OC; forward, 5′-CAGACAAGTCCCACACAGCA-3′ and reverse, 5′-CTTTATTTTGGAGCTGCTGT-3′), and mouse HPRT housekeeping gene (forward 5′-AGTGTTGGATACAGGCCAGAC-3′ and reverse, 5′-CGTGATTCAAATCCCTGAAGT-3′)were purchased from Invitrogen. All of the primer pairs used amplified a single band with the expected molecular weight as analyzed by agarose gel electrophoresis. The quantities of all samples were normalized to the mouse HPRT housekeeping gene.

Statistical Analysis

Results are presented as means ± SD. The differences between *th3/+* mice and age-matched WT controls were evaluated by Student's T-test. The differences between *th3/th3* mice, IR controls and WT controls were evaluated by one-way analysis of variance. Because of small

sample size, we were unable to assess the effect of sex on the observed parameters, but initial comparisons to sex-and age-matched controls consistently confirmed the observations in each group of animals. Statistical analysis was performed using the STATA software. Differences with *p*-values less than 0.05 were considered significant.

Results

i) Bone abnormalities of the *th3/+* and *th3/th3* mice

At age 4 mo, the *th3/+* mouse demonstrated moderate anemia (mean Hb was 7.7 ± 0.6 g/dl in the *th3/+* mice compared to 12. 3 ± 1.3 g/dl in WT, p<0.01). *Th3/th3* mice were studied at age 4mo (2 mo after transplantation) and results were compared to 4mo WT and IR controls (2mo after transplantation). As expected, the mean Hb of the *th3/th3* mice was extremely low, 1.1 ± 0.4 g/dl, compared to 11.3 ± 1.5 g/dl in IR mice and 12.5 ± 2.0 g/dl in WT(p<0.001).

Liver and spleen iron content were increased in the *th3/+* mice compared to WT. (Liver: 1.8 ± 0.14 vs. 0.35 ± 0.04 mcg/mg/dry weight; *th3/+* vs. WT, mean ± SD; p< 0.001. Spleen: 7.5 ± 1.2 vs. 4.4 ± 1.4 mcg/mg/dry weight; *th3/+* vs. WT, p< 0.001). Liver iron content was also increased in the *th3/th3* mouse (4.4 ± 0.4 mcg/mg/dry weight) compared to IR (0.3 ± 0.02 mcg/mg dry weight)and WT (0.36 ± 0.04 mcg/mg dry weight), p<0.001. However, spleen iron content of the *th3/th3* mice was the same as controls (3.95 ± 1.2 vs. 3.5 ± 1.5 vs. 4.4 ± 1.5 mcg/mg/dry weight, *th3/th3* vs. IR vs. WT). These results suggest differences in tissue iron distribution between the *th3/+* and *th3/th3* mouse.

μCT analysis identified similar trabecular abnormalities in both thalassemia mice (Table 1). These included decreased bone volume fraction (BV/TV), number of trabeculae (Tb.No.) and trabecular thickness (Tb.Th.)in both *th3/+* and *th3/th3* compared to their respective controls. Irradiation was found to have an intermediate effect on trabecular bone, with the μCT values of the IR animals plotting between the values seen in WT and *th3/th3* mice. However, trabecular changes in the *th3/th3* mice remained significantly different from those in IR animals.

Analysis of cortical bone (mid-diaphysis femur) in the *th3/+* mouse showed decreased cortical thickness and cortical area, and increased marrow area and inner perimeter compared to controls (Table 1). Cortical bone analysis of the *th3/th3* mouse did not differ from WT or IR controls. This is not surprising as this mouse was generated at age 2 months, when a great part of bone growth and accrual had been accomplished.

Changes in bone composition and material properties were determined by FTIRI. The spectroscopic parameters measured were Min/Matrix and Carb/Min ratios and collagen crosslinks. No difference was found in the mean values of these FTIR parameters between thalassemic mice and controls. Typical images of cortical sections and their respective pixel histograms for the *th3/+* mouse at age 4 months are presented in Figure 1. Although, we did not detect statistically significant changes in the mean values of either cortical or cancellous bone FTIRI parameters, we saw qualitative differences in pixel distribution histograms between affected and control animals, with the widths of the distribution increased in the thalassemic mice.

Biomechanical properties were tested by three point bending. Femurs of *th3/+* and *th3/th3* mice showed decreased maximum load, maximum moment and stiffness compared to their controls indicating increased fragility(Table 2). Similar to our μCT results, irradiation was found to have an effect on biomechanical properties, with values plotting between those of WT and *th3/th3* animals.

Histomorphometry showed decreased MAR and BRF in both *th3/+* and *th3/th3* mice compared to controls. In addition, we found decreased BV/TV (%), decreased Osteoid Surface (% BS) and decreased Octeoclast number for BS (no./mm) in both thalassemia mice(Figure 2). These results indicate decreased bone formation and resoption in these animals. Similar to histomorphometry results, RT-PC R analysis of femur extracted mRNA of both *th3/+* and *th3/th3* mice and their respective controls was significant for decreased expression of CTK and OC ($p < 0.01$; Figure 3), indicating again decreased bone turnover. Of note, both histomorphometry and RT-PCR data support an increase in bone turnover in the IR animals compared to non-irradiated WT controls.

ii) Longitudinal studies of the *th3/+* mouse

To determine longitudinal changes in thalassemia, we performed μCT analysis of trabecular and cortical bone of the *th3/+* mouse and age and sex matched controls at ages 2, 4, 6 and 9 months. The percent change in μCT parameters of the *th3/+* mouse compared to controls was calculated at each time point and presented at Figure 4 as percent of baseline. We found that μCT abnormalities are present by age 2 months, and do not worsen by 9 mo of age. Data on Hb concentrations and liver and spleen iron content in these animals at various time points are shown in Table 3. The severity of anemia remained the same over the 9 month period, while tissue iron content appeared to plateau after 4 months.

Discussion

In this study, we determined the bone abnormalities of the *th3* and *th3/th3* thalassemia mice. The *th3/+* mouse has mild-to-moderate anemia and splenomegaly, and thus represents a model of beta TI. The *th3/th3* model has lethal hemolysis comparable to beta TM. Both *th3/+* and *th3/th3* mice had similar trabecular abnormalities, characterized by a decreased number of trabeculae and increased trabecular spacing. Cortical bone abnormalities were present only in the *th3/+* mouse, and were significant for an increased bone marrow area and thinner cortices. Both models had changes in biomechanical properties suggestive of increased fragility. Overall, the bone abnormalities of the *th3* thalassemia mouse were reminiscent of the changes that have been traditionally described in patients with the disease.

We must acknowledge that besides differences in the severity of hemolysis there are additional characteristics that distinguish *th3/+* and *th3/th3* mice. These features may influence the bone phenotype as well as affect the use of these models in further studies of bone disease in thalassemia. *Th3/th3* animals are generated via transplantation of wild-type mice at an age when normal bone development has been largely achieved. They die of anemia in the relative short period of 8 to 10 weeks, which may affect the severity of the bone abnormalities that we observe. Their short lifespan does not allow for easy manipulation of the model or therapeutic interventions. It is likely, therefore, that the absence of cortical bone abnormalities in the *th3/th3* mouse is related to model limitations rather than to thalassemia itself. The assessment of bone changes in the *th3/th3* mouse is further complicated by the effect of total body irradiation on the bone. To account for this limitation, the results of the *th3/th3* mouse were compared to both WT and irradiated controls. Irradiation had a detectable effect on trabecular μCT values. Nonetheless, the μCT results in *th3/th3* mice were significant even when compared to irradiated controls. There was also a trend towards decreased biomechanical properties in irradiated controls suggesting that the results of biomechanical testing in the *th3/th3* animals can be attributed in part to irradiation. On the other hand, the *th3/+* mouse has none of the above limitations and additionally has a normal lifespan, so that we can easily use it for longitudinal and other intervention studies. Finally, because of the small number of studied animals, we are unable

to comment on potential gender differences in these animal models. It also possible that the effect of irradiation on the bone was missed because of small sample size.

FTIRI analysis was performed to determine changes in the material composition of the bone, including mineralization relative to the collagen composition of the bone, hydroxyapatite structure and collagen maturity. Mean values in FTIRI parameters did not differ between the thalassemia mice and their controls. It is possible that the study was underpowered to detect small FTIR changes. However, we observed differences in the distribution of measured parameters among animal groups, which suggests differences in heterogeneity of the various chemical components that constitute a healthy bone structure [12,13]. Bone is heterogeneous due to constant remodeling, and differences in the rates of primary and secondary mineralization. Heterogeneity is thought to affect the mechanical properties of the bone[14]. Decreased heterogeneity in FTIR parameters, for example, has been observed with prolonged bisphosphonate treatment, which may contribute to the increased bone brittleness that has been described with such therapy[13].

Based on the longitudinal *th3/+* μCT data, the bone abnormalities are established by 2 months. There is no evidence of progressive bone loss at the subsequent 7 months. This is similar to what has been recently reported in patients with the disease. Specifically, peak bone mass is sub-optimal in patients with thalassemia, and loss of bone mass is more pronounced in children and adolescents compared to adults, indicating a primary problems with bone accrual [7].

Thalassemia is characterized by anemia and ineffective erythropoiesis, or otherwise, the production and subsequent destruction of large numbers of defective red blood cells and their precursors in the bone marrow[1]. Ineffective erythropiesis has been associated with the development of facial and long bone deformities in beta TM patients chronically maintained at low Hb levels[15]. These abnormalities resolve with regular transfusions that start early in life[15], confirming the role of ineffective erythropoiesis in such cases. However, the impact of ineffective erythropoiesis in the development of low bone mass despite the near normalization of Hb concentrations is unclear. Our data indicate that the ineffective erythropoiesis associated with mild to moderate anemia, such as seen in the *th3/+* mouse, is sufficient to cause changes in bone micro architecture and material properties and is associated with decreased bone turnover. Decreased bone turnover was indeed found in both *th3/+* and *th3/th3* mice. In addition to ineffective erythropoiesis, both mice have evidence of increased liver iron content. This is most likely related to increased gastrointestinal absorption of iron. As it has been recently shown, hepcidin, a negative regulator of intestinal iron absorption, is in appropriately suppressed in this model leading to increased iron absorption [16]. However, the iron overload that is seen typically in patients is much more severe and related primarily to repeated transfusions. Although we cannot rule out the fact that the degree of increased tissue iron that is found in the thalassemia mouse may be responsible for some of its bone abnormalities, the predominant pathologic process in these animals is ineffective erythropoiesis.

Bone turnover has been examined in adult patients with beta TM maintained on regular transfusions and iron chelation therapy. Contrary to our animal data, these patients have been described as having mildly increased resorption [17,18]. The effect of iron chelation on bone metabolism is largely unknown, and may contribute to the increased resorption in humans. Most of adults with beta TM have iron induced hypogonadism[19], which is known to be associated with increased resorption. Finally, differences in bone turnover between animals and humans may have to do with differences in the severity of iron overload. The role of iron excess in the development of osteoporosis in patients with thalassemia or hereditary hemochromatosis, a disease caused by mutations that increase intestinal iron

absorption, has yet to be confirmed because studies in humans yield inconsistent results[7,20]. Moreover, the role of iron overload on bone turnover is still unclear, with a single report documenting focal osteomalacia due to iron in poorly transfused and iron overloaded patients [21].

In summary, this study of mouse models of beta TI and beta TM documents changes in bone micro architecture and increased fragility analogous to what is seen in patients with the disease, and validates their use in further studies on osteoporosis in thalassemia. As in humans, the bone abnormalities present early in life indicating a defect in bone accrual. Both bone formation and resorption are decreased in these mice. Further studies are needed to document the role of iron on bone micro architecture and turnover, and to bring to light the factors that lead to the decreased bone turnover associated with ineffective erythropoiesis.

Acknowledgments

The authors thank Lyudmila Lukashova for assistance with the micro-CT, Mila Spevac for assistance with FTIR and Orla O'Shea for assistance with the histology. This work was supported by National Institutes of Health Grants KO8 HL 088231. The study utilized the Core Center facilities for Musculoskeletal Integrity at HSS (AR046121).

References

1. Rund D, Rachmilewitz. B-Thalassemia. NEJM 2005;353 (11):1135–1146. [PubMed: 16162884]
2. Calleja E, Shen JY, Lesser M, Grady RW, New MI, Giardina PJ. Survival and Morbidity in Transfusion Dependent Thalassemia Patients on Subcutaneous Desferrioxamine Chelation: Nearly Two Decades of Experience. NY Acad Sci 1998;850:469–470.
3. Vogiatzi MA, Macklin EA, Fung EB, Vichinsky E, Oliveri N, Kwiatkowski JL, Cohen A, Neufeld E, Giardina PJ. Prevalence of fractures among the Thalassemia syndromes in North America. Bone 2006;38:571–575. [PubMed: 16298178]
4. Domrongkitchaiporn S, Sirikulchayanonta V, Angchaisuksiri P, Stitchantrakul W, Kanokkantopong C, Rajatanavin R. Abnormalities in bone mineral density and bone histology in thalassemia. J Bone Mineral Research 2003;18(9):1682–1686.
5. Jensen CE, Tuck SM, Agnew JE, et al. High incidence of osteoporosis in Thalassemia major. Journal of Pediatric Endocrinology and Metabolism 1998;11:979–977. [PubMed: 10091177]
6. Pollak RD, Rachmilewitz E, Blumenfeld A, Idelson M, Goldfarb AW. Bone mineral metabolism in adults with B-thalassemia major and intermedia. British Journal of Haematology 2000;111:902–907. [PubMed: 11122154]
7. Vogiatzi MA, Macklin EA, Fung EB, Cheung AM, Vichinsky E, Oliveri N, Kirby M, Kwiatkowski JL, Cunningham M, Holm I, Lane J, Schneider R, Fleisher M, Grady RW, Peterson C, Giardina PJ. for the Thalassemia Clinical Research Network. Bone disease in thalassemia: a frequent and still unresolved problem. J Bone Miner Res 2009;24(3):543–57. [PubMed: 18505376]
8. Rivella S, May C, Chadburn A, Riviere I, Sadelain M. A novel murine model of Cooley anemia and its rescue by lentiviral-mediated human beta-globin gene transfer. Blood 2003;101:2932–2939. [PubMed: 12480689]
9. Boskey AL, Pleshko N, Doty SB, Mendelsohn R. Applications of Fourier transform infrared (FT-IR) microscopy to the study of mineralization in bone and cartilage. Cells Materials 1992;2:209–220.
10. Boskey AL, Mendelsohn R. Infrared spectroscopic characterization of mineralized tissues. Vibrat Spectrosc 2005;38:107–114.
11. Paschalis EP, Verdelis K, Mendelsohn R, Boskey A, Yamauchi M. Spectroscopic determination of collagen cross-links in bone. J Bone Miner Res 2001;16:1821–1828. [PubMed: 11585346]
12. Gourion-Arsiquaud S, Faibish D, Myers E, Spevak L, Compston J, Hodsman A, Shane E, Recker RR, Boskey ER, Boskey AL. Use of FTIR Spectroscopic Imaging to Identify Parameters Associated With Fragility Fracture. J Bone Miner Res 2009;2009(24):1565–1571. Published online on April 27, 2009. 10.1359/JBMR.090414 [PubMed: 19419303]

13. Boskey AL, Spevak L, Weinstein RS. Spectroscopic markers of bone quality in alendronate-treated postmenopausal women. Osteoporos Int 2009;20:793–800.10.1007/s00198-008-0725-9 [PubMed: 18769963]

14. Ruffoni D, Fratzl P, Roschger P, Klaushofer K, Weinkamer R. The bone mineralization density distribution as a fingerprint of the mineralization process. Bone 2007;40 (5):1308–1319. [PubMed: 17337263]

15. Piomelli S, Danoff SJ, Becker MH, Lipera MJ, Travis SF. Prevention of bone malformations and cardiomegaly in Cooley's anemia by early hypertransfusion regimen. Annals of the NY Academy of Science 1969;165:427–436.

16. Gardenghi S, Marongiu MF, Ramos P, Guy E, Breda L, Chadburn A, Liu Y, Amariglio N, Rechavi G, Rachmilewitz EA, Breuer W, Cabantchik ZI, Wrighting DM, Andrews NC, de Sousa M, Giardina PJ, Grady RW, Rivella S. Ineffective erythropoiesis in beta-thalassemia is characterized by increased iron absorption mediated by down-regulation of hepcidin and up-regulation of ferroportin. Blood 2007;109(11):5027–5035. [PubMed: 17299088]

17. Voskaridou E, Kyrtsonis MC, Tempos E, Skordili M, Theodoropoulos I, Bergele A, Diamanti E, Kalovidoulis A, Loutradi A, Loukopoulos D. Bone resorption is increased in young adults with thalassemia major. British Journal of Haematology 2001;112:36–14. [PubMed: 11167780]

18. Lasco A, Morabito N, Gaudio A, Buemi M, Wasniewska M, Frisina N. Effects of hormonal replacement therapy on bone metabolism in young adults with beta-thalassemia major. Osteoporos Int 2001;12(7):570–5. [PubMed: 11527055]

19. Vogiatzi MG, Macklin EA, Trachtenberg FL, Fung EB, Cheung AM, Vichinsky E, Olivieri N, Kirby M, Kwiatkowski JL, Cunningham M, Holm IA, Fleisher M, Grady RW, Peterson CM, Giardina PJ. Thalassemia Clinical Research Network. Differences in the prevalence of growth, endocrine and vitamin D abnormalities among the various thalassaemia syndromes in North America. Br J Haematol Sept 2009;146(5):546–56. Epub 2009 Jul 13.

20. Guggenbuhl P, Deugnier Y, Boisdet JF, Rolland Y, Perdriger A, Pawlotsky Y, Chalès G. Bone mineral density in men with genetic hemochromatosis and HFE gene mutation. Osteoporosis international 2005;16 (12):1809–14. [PubMed: 15928800]

21. Mahachoklertwattana P, Sirikulchayanonta V, Chuansumrit A, Karnsombat P, Choubtum L, Sriphrapradang A, Domrongkitchaiporn S, Sirisriro R, Rajatanavin R. Bone histomorphometry in children and adolescents with beta-thalassemia disease: iron-associated focal osteomalacia. J Clin Endocrinol Metab 2003;88(8):3966–72. [PubMed: 12915694]

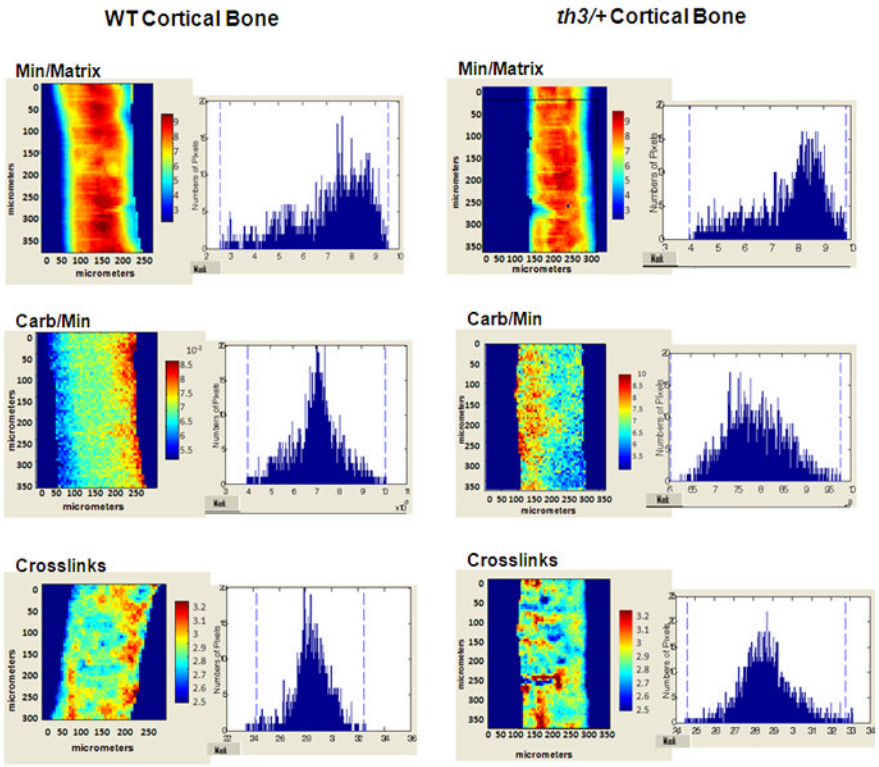

Figure 1.
Typical FTIR images of cortical sections of the th3/+ mice and their controls at age 4 months. Pixel histograms adjacent to the figures illustrate the data distribution in the images shown. Changes in distribution between affected and WT animals indicate differences in material properties. Min/Matrix mineral-to-matrix ratio, Carb/Min carbonate-to-mineral ratio

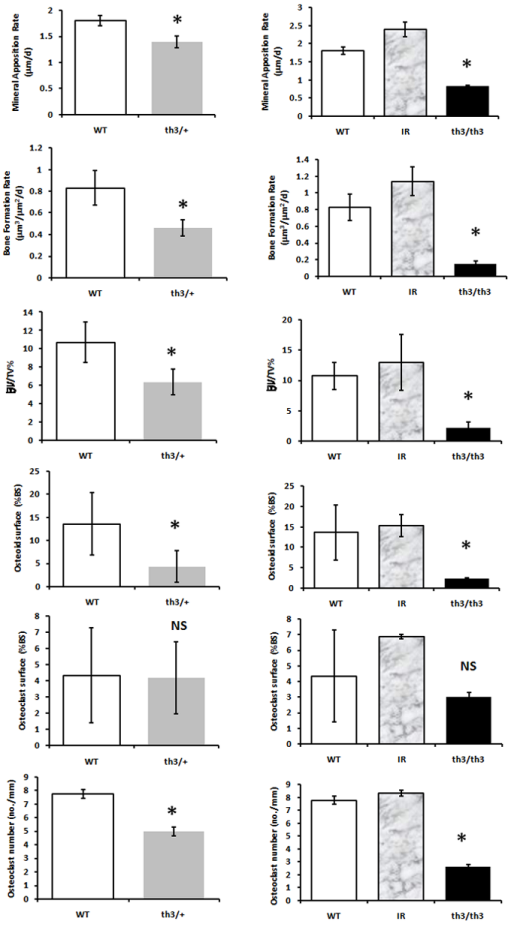

Figure 2.

Histomorphometry indicates decreased bone formation and resorption in both th3/+ and th3/th3 mice compared to their controls. Calcein (100 mg/kg body weight) and xylenol orange (90 mg/kg body weight) were injected at 7 and 3 days, respectively, prior to death. Double- and single-labeled perimeters and interlabel width of double-labeled regions were measured. The mineral apposition rate (MAR, μm/day) and bone formation rate (BFR/BS, μm3/μm2/day) were then determined. Longitudinal femur sections were also stained using the von Kossa method and Goldner's trichrome. Trabecular bone volume (BV/TV, %), osteoclast surface, and osteoid surface for bone surface (BS) were measured. Paraffin-embedded longitudinal femur sections were stained for TRAP. Osteoclast number per BS (n/mm) was the determined. All measurements were done using the Bioquant program. WT wild-type, shown as white bars; IR irradiated control, shown as gray-patterned bars; th3/+ shown as gray bars; th3/th3 shown as black bars. *$P < 0.05$

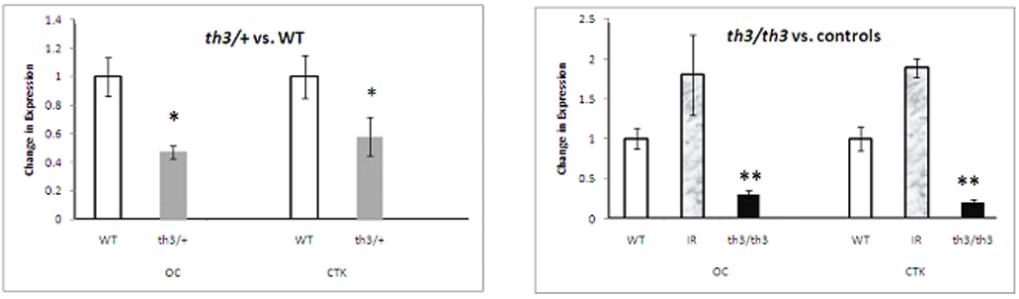

Figure 3.

Decreased cathepsin K and osteocalcin expression in both th3/+ and th3/th3 mice compared to controls. Total mRNA was prepared from femurs after bone marrow was flushed. Levels of expression were normalized to the mouse HPRT housekeeping gene. Values are expressed as mean ± SD. WT wild-type, shown as white bars; IR irradiated control, shown as gray-patterned bars; th3/+ shown as gray bars; th3/th3 shown as black bars. *P < 0.05, **P < 0.01

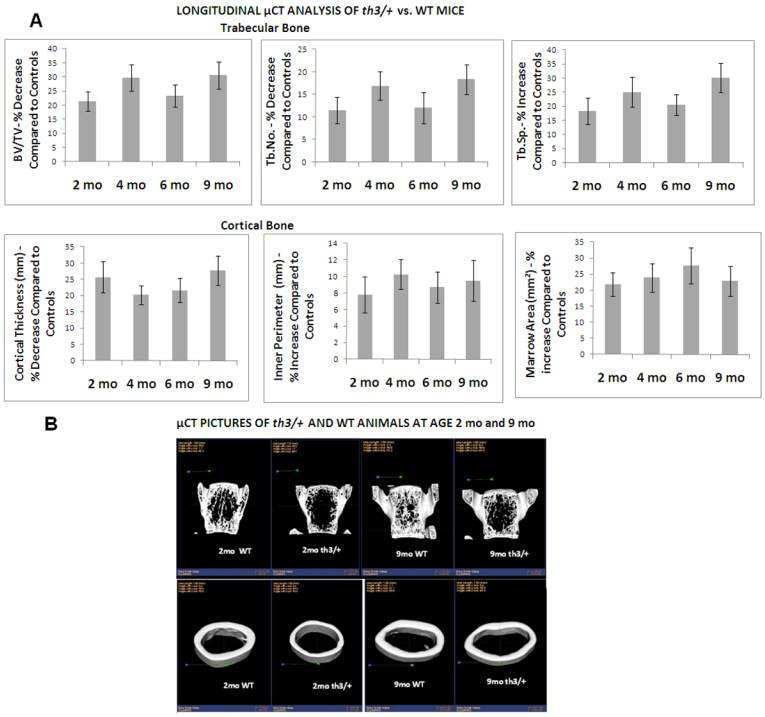

Figure 4.

Longitudinal µCT analysis of th3/+ mice. a µCT analysis of trabecular (first row) and cortical (second row) bone. Percent increase or decrease of various µCT parameters of th3/+ animals compared to age-matched controls was calculated. Animals were studied at ages 2, 4, 6, and 9 months (n = 6/group). µCT changes were present by 2 months and did not worsen by 9 months. Error bars represent SDs. b Representative µCT images of th3/+ and their controls at 2 and 9 months: vertical sections of vertebral body at L5 (first row) and cortical bone at mid-diaphysis femor (second row). Affected animals manifest thinning of trabeculae and thinner cortices. Comparison of images at 2 and 9 months does not indicate progressive disease, indicating that these bone abnormalities develop early during the period of bone accrual

Table 1

μCT analysis of *th3/+* and *th3/th3* mice compared to their controls at age 4 months.

	th3/+	**WT**	***th3/th3***	**IR**	**WT**
Trabecular bone					
BMD (mg/mm^3)	792 ± 10	837 ± 18*	797 ± 25	820 ± 9.5	825 ± 21*
BV/TV (%)	13.9 ± 2.4	19.7 ± 1.8*	12.1 ± 2.3	16.4 ± 2.5	18.2 ± 1.6*
Trabecular Number (N/mm)	4.13 ± 0.6	4.97 ± 0.6**	3.98 ± 0.1	4.35 ± 0.3	4.90 ± 0.7**
Trabecular Thickness (μm)	41.6 ± 4	48.7 ± 3**	40.9 ± 3	48.7 ± 3	49.3 ± 2*
Trabecular Spacing (μm)	275 ± 38	220 ± 35†	281 ± 44	248 ± 25	229 ± 27 **
Cortical Bone					
Cortical thickness (mm)	0.14 ± 0.007	0.18 ± 0.008**	0.16± 0.01	0.16 ± 0.005	0.19 ± 0.01
Inner Perimeter (mm)	4.2 ± 0.1	3.8 ± 0.2**	3.9 ± 0.1	3.7 ± 0.15	3.8 ± 0.1
Outer Perimeter (mm)	4.5 ± 0.1	4.8 ± 0.2†	4.7 ± 0.1	4.8 ± 0.3	4.7 ± 0.3
Cortical Area (mm^2)	0.61 ± 0.04	0.75 ± 0.03**	0.69 ± 0.01	0.70 ± 0.02	0.70 ± 0.03
Marrow Area (mm^2)	1.15 ± 0.09	0.9 ± 0.1**	0.9 ± 0.1	0.95 ± 0.2	0.94 ± 0.2

*P<0.01;

**p<0.05

†p=trend

Values are expressed as mean ± SD

WT: wild type control; IR: irradiated control

Table 2

Biomechanical properties of the femurs from *th3/+* and *th3/th3* mice compared to controls at age 4 months.

	Maximum Load (N)	Maximum Moment (Nmm)	Stiffness (N/mm)
th3/+	15.54 ± 2.56 *	27.20 ± 4.49 *	106 ± 19 *
WT	20.37 ± 2.90	35.64 ± 5.00	135 ± 24
th3/th3	15.30 ± 2.45 *	26.77 ± 4.29 *	92 ± 18 *
IR	17.27 ± 2.75	30.23 ± 4.82	112 ± 18
WT	20.37 ± 2.90	35.64 ± 5.00	135 ± 24

* $p < 0.01$;

Values are expressed as mean ± SD

WT: wild type control

IR: irradiated control.

Table 3

Hemoglobin (Hb) and liver and spleen iron concentrations in *th3/+* mice compared to controls at age 2, 4, 6 and 9 months.

		Hb (g/dl)	Liver iron (mcg/mg dw)	Spleen iron (mcg/mg dw)
2 mo	***th3/+***	7.1 ± 0.6*	1.22 ± 0.06**	4.44 ± 0.85
	WT	12.3 ± 1.3	0.40 ± 0.03	2.79 ± 2.12
4 mo	***th3/+***	7.7 ± 0.6*	1.8 ± 0.14**	7.53 ± 1.22**
	WT	12.3 ± 1.3	0.35 ± 0.04	4.4 ± 1.43
6 mo	***th3/+***	6.9 ± 0.8*	1.28 ± 0.12**	7.03 ± 1.31*
	WT	12.0 ± 1.8	0.33 ± 0.05	3.23 ± 2.52
9 mo	***th3/+***	7.7 ± 0.4*	1.82 ± 0.15**	6.87 ± 1.02*
	WT	13.3 ± 1.8	0.37 ± 0.05	3.52 ± 1.89

* $p < 0.01$;

** $p < 0.001$

Values are expressed as mean ± SD

WT: wild type control

dw: dry weight